

¹ prosail: an R package to simulate canopy reflectance
² with the coupled model PROSAIL (PROSPECT +
³ SAIL)

⁴ Jean-Baptiste Féret  ¹ and Florian de Boissieu  ¹

⁵ 1 TETIS, INRAE, AgroParisTech, CIRAD, CNRS, Université Montpellier, Montpellier, France 
⁶ Corresponding author

DOI: [10.xxxxxx/draft](https://doi.org/10.xxxxxx/draft)

Software

- [Review](#) 
- [Repository](#) 
- [Archive](#) 

Editor: 

Submitted: 31 January 2026

Published: unpublished

License

Authors of papers retain copyright and release the work under a Creative Commons Attribution 4.0 International License ([CC BY 4.0](https://creativecommons.org/licenses/by/4.0/)).

Summary

The PROSAIL model is a widely used radiative transfer model that combines the *leaf optical PROPERTIES SPECtra* (PROSPECT) model with the *Scattering by Arbitrarily Inclined Leaves* (SAIL) canopy bidirectional reflectance model (Berger et al., 2018; Jacquemoud et al., 2009). It is designed to simulate the reflectance of vegetation canopies across a broad spectral domain, including the visible, near-infrared, shortwave infrared and thermal infrared regions of the electromagnetic spectrum.

PROSAIL integrates the optical properties of individual leaves, calculated by PROSPECT (Jacquemoud & Baret, 1990), with the structural characteristics of the canopy modeled by SAIL (W. Verhoef, 1984). This combination allows for the simulation of how light interacts with vegetation at both the leaf and canopy levels, taking into account factors such as leaf chemical content, leaf structure, canopy architecture, and viewing and illumination angles.

PROSAIL's ability to simulate plant canopy spectral and directional reflectance under various conditions makes it a valuable tool for agricultural monitoring, ecological studies, and climate research, where PROSAIL can be used to simulate vegetation optical properties (Poulter et al., 2023). It is also used in combination with inversion procedures to retrieve vegetation biophysical properties. These biophysical properties include leaf area index (LAI), leaf water and pigment content, the fraction of absorbed photosynthetically active radiation (fAPAR), albedo and fractional vegetation cover (fCover) among others. The capacity to retrieve a biophysical property mainly depends on the spectral characteristics of the sensor, and the acquisition of sufficient spectral information to solve an ill-posed problem.

Here, we introduce prosail, an R package which provides multiple versions of the model PROSAIL, coupled with the latest versions of PROSPECT distributed with the R package prospect (Féret & Boissieu, 2024). The package includes functions to run simulations of surface reflectance in forward mode for various optical sensors, as well as functions to apply user defined spectral response function (SRF), allowing simulation of any optical sensor with known or approximated surface reflectance. It also includes functions for model inversion using iterative optimization with and without prior information, as well as a module dedicated to hybrid inversion, combining physical modeling and machine learning regression, applicable to data tables and raster data.

Statement of need

The capacity to measure, map and monitor vegetation traits corresponding to biophysical and chemical properties is crucial to better understand ecosystem and agrosystem functions, as

well as carbon, water and energy budgets. Vegetation radiative transfer models (RTMs) aim at describing the interactions between light and these biophysical and chemical properties, through absorption and scattering mechanisms. At leaf scale, the model PROSPECT ([Féret & Boissieu, 2024](#)) is currently the most popular physical model for the simulation of leaf optical properties and the accurate estimation of leaf chemistry ([Féret et al., 2019; Spafford et al., 2021](#)). At canopy scale, various models can be employed, and the choice for a specific model may be driven by the complexity of the system to be simulated, as well as the capacity to describe the scene.

The SAIL model is an example of four-stream representations of the radiative transfer equation, including two direct fluxes (incident solar flux and radiance in the viewing direction) and two diffuse fluxes (upward and downward hemispherical flux). A system of four linear differential equations can then be analytically solved. Detailed description of the functioning of the different SAIL versions can be found in ([Wout Verhoef & Bach, 2007](#)) and ([W. Verhoef et al., 2007](#)).

More complex models include the *Soil Canopy Observation of Photosynthesis and Energy fluxes* (SCOPE) ([Yang et al., 2021](#)) model, which features layered description of the vegetation, enabling the simulation of vegetation with an understorey or with a vertical gradient in leaf properties, and the *Discrete Anisotropic Radiative Transfer* DART model ([Gastellu-Etchegorry et al., 2015](#)), which allows for explicit 3-dimensional description of the canopy using geometric representations with triangular meshes or turbid voxels that can be derived from LiDAR acquisitions.

RTMs are increasingly used in remote sensing applications, in combination with machine learning: RTMs are used to produce a surface reflectance dataset with corresponding vegetation properties, which are then used as training data to adjust a regression model with a machine learning algorithm. Such strategies, commonly referred to as hybrid methods ([Verrelst et al., 2015](#)), show multiple advantages : simulations are used in place of extensive in situ sampling, allowing regression model adjustment on virtually any source of optical imagery and any training sample size, while the use of machine learning ensures computation efficiency compared to iterative optimization when processing imagery data.

The relatively limited number of input parameters and the computational efficiency of the SAIL model makes it particularly interesting for operational applications, despite the main assumption of vegetation as a homogeneous turbid medium, where leaves are randomly distributed within the canopy, which is not accurate for row crops and heterogeneous canopies.

State of the field

Various softwares currently provide procedures for hybrid inversion with PROSAIL simulations. The *Sentinel Toolbox Application Platform* (SNAP) includes the Biophysical Processor module ([Weiss et al., 2020](#)), which provides an implementation of PROSAIL hybrid inversion combining PROSAIL simulations with an artificial neural network regression model, for the estimation of vegetation properties, such as LAI, fAPAR, fcover, canopy chlorophyll content and canopy water content. The sampling strategy for the definition of the training set, including the distribution and co-distribution of the input parameters, is described in the *Algorithmic Theoretical Background Document* (ATBD) ([Weiss et al., 2020](#)) and cannot be adjusted by users. Alternative distributions provide more interactive parameterization of the inversion strategy, such as the *Automated Radiative Transfer Models Operator* (ARTMO) toolbox ([Caicedo et al., 2014](#)) developed in Matlab.

The R package prosail includes the versions of the model PROSPECT implemented in the package prospect: PROSPECT-D ([Féret et al., 2017](#)) and PROSPECT-PRO ([Féret et al., 2021](#)). It also includes two versions of the model SAIL:

- 4SAIL ([W. Verhoef et al., 2007](#)), a numerically stable adaptation of the SAILH version

89 (W. Verhoef, 1998), which incorporate foliage hot spot to the original SAIL model

90 ▪ **4SAIL2** (Wout Verhoef & Bach, 2007), a two layers version of 4SAIL accommodating

91 horizontal and vertical heterogeneities. This version includes additional parameters to

92 account for crown clumping, and to describe the vertical distribution of two types of leaves

93 described by specific leaf optical properties, which may describe different phenological

94 stages or different vegetation types.

The R package prosail also provides a set of functions to help researchers aiming at experimenting for the estimation vegetation biophysical properties from optical remote sensing using RTM with open-source solutions. These functions include :

- the simulation of surface reflectance for any optical sensor based on their SRF
 - the production of look-up-tables (LUTs) for simulated sensor surface reflectance and corresponding PROSAIL input parameters, with or without additive and multiplicative noise
 - the application of iterative optimization with possible added prior information on data tables
 - the application of hybrid inversion on data tables and raster data

The package prosail does not intend to provide the same computational efficiency as SNAP. It does not provide a collection of models and methods as comprehensive as those provided with the ARTMO box neither. prosail provides a flexible open source framework to experiment with hybrid inversion procedures, using simple yet fast and efficient training stage, allowing experimenting on strategies for training data sampling, introduction of noise, feature selection over any type of optical sensor. It is particularly suitable for research and development, in order to identify potential and limitations of inversion strategies and parameterizations. Resulting regression models can be applied on remote sensing data, but it may not be the appropriate software for scaling up vegetation monitoring applications.

114 Alternative PROSAIL implementations can be found at [this webpage](#). This includes distributions
115 in matlab, python and fortran programming languages. Note that alternative PROSAIL
116 implementations are also available in packages written in [python](#), [Julia](#) and [R](#).

117 Software design

prosail uses the R package `prospect` ([Féret & Boissieu, 2024](#)) for the simulation of leaf optical properties. It provides a user-friendly and modular set of functions, in order to run simulations of vegetation canopy reflectance, and to predict vegetation biophysical properties using various inversion strategies. Model inversion is a multi-step procedure requiring simulation of sensor reflectance in order to train a machine learning regression algorithm, then applicable to any new data source, including raster data from airborne and spaceborne sensors.

- The generation of realistic reflectance simulations requires definition of input parameter sampling strategy, accounting for sensor SRF and uncertainties. prosail provides functions to produce this training dataset as a unique step following standard parameterization, or step by step, in order for users to understand the logic, or adjust each step to their needs.
 - A limited number of machine learning algorithms is currently provided, but the software design will allow integration of additional algorithms in future versions.
 - Raster processing is mainly handled with the terra ([Hijmans, 2025](#)) package, to ensure compatibility with most raster data formats.
 - prosail can be used in combination with `preprocS2`, a package dedicated to downloading and preprocessing of Earth observation data following the [STAC](#) specification, in order

135 to produce a fully automated image access and processing workflow.

136 Research impact statement

137 prosail has been used in multiple research publications since its early developments ([Hauser et](#)
138 [al., 2021](#)), ([Ferreira et al., 2026](#)), ([Féret et al., 2026](#)). It is currently used in multiple research
139 projects, and is actively maintained.

140 Overview

141 PROSAIL simulation in forward mode

142 PROSAIL requires information intrinsic to vegetation :

- 143 ▪ leaf optical properties, including leaf directional hemispherical reflectance and
144 transmittance. These leaf optical properties are simulated with the R package prospect
145 ([Féret & Boissieu, 2024](#)) and readers are invited to refer to the documentation of this
146 package for a comprehensive description of the leaf chemical and structure parameters
147 accounted for by the various versions of the PROSPECT model. Measured leaf optical
148 properties can also be used instead of simulated ones.
- 149 ▪ LAI, which is defined as the one-sided green leaf area per unit ground surface area in
150 broadleaf canopies. It is dimensionless and is sometimes expressed in $m^2.m^{-2}$
- 151 ▪ Leaf inclination distribution, which can be defined following different *Leaf Inclination*
152 *Distribution Functions* (LIDF). The LIDF used in the original version of SAIL
153 [[verhoef1998](#)] describes leaf inclination based on two parameters: lidf_a controls the
154 average leaf slope, and lidf_b controls the distribution's bimodality. Both parameters
155 should be set between -1 and 1 and the sum of absolute values inferior to 1. An
156 alternative LIDF defined by ([Campbell, 1990](#)) can be applied, and requires a unique
157 parameter corresponding to the average leaf angle.
- 158 ▪ a foliage hot spot parameter which corresponds to the ratio of the correlation length
159 of leaf projections in the horizontal plane and the canopy height ([Bréon et al., 2002](#);
160 [Kuusk, 1991](#); [Wout Verhoef & Bach, 2007](#))

161 PROSAIL also requires information extrinsic to vegetation :

- 162 ▪ the sun-observer geometry, defined by the sun zenith angle, the observer zenith angle,
163 and the relative azimuth angle between sun and observer
- 164 ▪ the soil reflectance

165 Additional parameters are required to run the version 4SAIL2 :

- 166 ▪ the optical properties corresponding to the second type of leaves
- 167 ▪ the fraction of LAI corresponding to a second type of leaves
- 168 ▪ a layer dissociation factor between the main leaf layer and the second leaf layer
- 169 ▪ the vertical crown cover percentage, which corresponds to the percentage of ground area
170 covered with crowns as seen from nadir direction
- 171 ▪ a tree shape factor corresponding to the ratio of crown diameter to crown height

172 SAIL produces a list of output variables corresponding to four top-of-canopy reflectance factors.
173 Additional parameters required to compute albedo, fAPAR and fcover are also provided as
174 outputs. The full list of outputs is then :

- 175 ▪ rddt: bi-hemispherical reflectance factor

```

176     ▪ rsdt: directional-hemispherical reflectance factor for solar incident flux
177     ▪ rdot: hemispherical-directional reflectance factor in viewing direction
178     ▪ rsot: bi-directional reflectance factor
179     ▪ abs_dir: canopy absorptance for direct solar incident flux
180     ▪ abs_hem: canopy absorptance for hemispherical diffuse incident flux
181     ▪ fcover: Fraction of green Vegetation Cover (equals to 1 - beam transmittance in the
182       target-view path)
183     ▪ rsdstar: contribution of direct solar incident flux to albedo
184     ▪ rddstar: contribution of hemispherical diffuse incident flux to albedo
185 The function prosail using 4SAIL can be called as follows :

```

```

# Load prosail package
library(prosail)

# define PROSPECT input variables. Refer to prospect tutorial for default values
input_prospect <- data.frame('chl' = 40, 'car' = 8, 'ant' = 0.0,
                             'ewt' = 0.01, 'lma' = 0.009, 'n_struct' = 1.5)

# define input variables for SAIL.
lai <- 5          # LAI
hotspot <- 0.1    # foliage hot spot parameter
type_lidf <- 2    # leaf inclination distribution function : Campbell
lidf_a <- 30      # average leaf angle (degrees)
tts <- 30         # geometry of acquisition: sun zenith angle (degrees)
tto <- 10         # geometry of acquisition: observer zenith angle (degrees)
psi <- 90          # geometry of acquisition: sun-observer azimuth (degrees)
rsoil <- spec_soil_oss$soil_01 # soil reflectance selected from OSSL library

# run PROSAIL with 4SAIL
ref_4sail <- prosail(input_prospect = input_prospect,
                      type_lidf = type_lidf, lidf_a = lidf_a, lai = lai,
                      hotspot = hotspot, tts = tts, tto = tto, psi = psi,
                      rsoil = rsoil)

```

```

186 Additional input variables are required when using 4SAIL2 :

```

```

# define leaf chemical content corresponding to two types of leaves
input_prospect <- data.frame('chl' = c(40,5), 'car' = c(8,5), 'ant' = c(0,1),
                             'ewt' = c(0.01,0.005), 'lma' = c(0.009,0.008),
                             'brown' = c(0.0,0.5), 'n_struct' = c(1.5,2))

# define additional 4SAIL2 parameters
fraction_brown <- 0.5    # fraction of LAI corresponding to second type of leaves
diss <- 0.5                 # layer dissociation factor between the leaf layers
cv <- 1                     # vertical crown cover percentage
zeta <- 1                   # tree shape factor

# run PROSAIL with 4SAIL2
ref_4sail2 <- prosail(SAILversion = '4SAIL2', input_prospect = input_prospect,
                      type_lidf = type_lidf, lidf_a = lidf_a, lai = lai,
                      hotspot = hotspot, tts = tts, tto = tto, psi = psi,

```

```
rsoil = rsoil, fraction_brown = fraction_brown,
diss = diss, cv = cv, zeta = zeta)
```

187 Computation of surface reflectance from PROSAIL outputs

188 The surface reflectance results from the combination of hemispherical-directional and bi-
 189 directional reflectance factors with the relative contribution of direct and diffuse radiation. The
 190 direct and diffuse radiations are defined as described by (C. François et al., 2002). Users can
 191 then compute surface reflectance by setting a global contribution of diffuse skylight radiation
 192 with the skyl parameter, which is the share of diffuse flux in global radiation. Alternatively,
 193 the direct and diffuse radiations can be taken into account by computing skyl based on the
 194 equation proposed by (Spitters et al., 1986), knowing the sun zenith angle and assuming clear
 195 sky conditions.

```
# Compute surface reflectance with known skyl
surf_refl_4sail <- get_surf_refl(rdot = ref_4sail$rdot,
                                 rsot = ref_4sail$rsot,
                                 skyl = 0.23,
                                 spec_atm_sensor = spec_atm)

# Compute surface reflectance using sun zenith angle (clear sky conditions)
surf_refl_4sail <- get_surf_refl(rdot = ref_4sail$rdot,
                                 rsot = ref_4sail$rsot,
                                 tts = 40,
                                 spec_atm_sensor = spec_atm)
```

196 Computation of fAPAR and albedo

197 The fAPAR in the direction of the observer can be computed by combining both canopy
 198 absorptance for direct solar incident flux and canopy absorptance for hemispherical diffuse
 199 incident flux.

```
fapar_4sail <- get_fapar(abs_dir = ref_4sail$abs_dir,
                           abs_hem = ref_4sail$abs_hem,
                           tts = tts, spec_atm_sensor = spec_atm)
```

200 Finally, the albedo can be derived from direct solar incident flux and hemispherical diffuse
 201 incident flux.

```
albedo_4sail <- get_albedo(rsdstar = ref_4sail$rsdstar,
                            rddstar = ref_4sail$rddstar,
                            tts = tts, spec_atm_sensor = spec_atm)
```

202 Simulating surface reflectance acquired by a sensor

203 The simulation of sensor surface reflectance requires the SRF of the sensor. A selection of
 204 SRF corresponding to multiple sensors is already implemented in prosail :

- 205 ▪ Sentinel-2A, 2B and 2C
- 206 ▪ Landsat-7, 8 and 9
- 207 ▪ MODIS
- 208 ▪ Venus
- 209 ▪ SPOT-6 / 7
- 210 ▪ Pleiades 1

211 Users can also define the sensor of their choice, either by providing central wavelength and full
 212 width at half maximum (fwhm) corresponding to each band and assuming gaussian response
 213 for each band, or by providing a file describing the exact SRF.

```
# get the spectral response function (SRF) for Sentinel-2A
srf_s2 <- get_srf_sensor(sensor_name = 'Sentinel_2A')

# get the SRF corresponding to a sensor defined by user.
# Hyperspectral sensor: 10 nm spectral sampling & 10 nm fwhm for all bands
wl <- seq(400, 2500, by = 10)
fwhm <- rep(x = 10, length = length(wl))
spectral_props = data.frame(wl = wl, fwhm = fwhm)
sensor_name <- 'Hyperspectral_Sensor'
srf_hsi <- get_srf_sensor(sensor_name = sensor_name,
                           spectral_properties = spectral_props)
```

214 PROSAIL inversion through iterative optimization

215 Iterative optimization with no prior information

216 PROSAIL is a relatively simple and computationally efficient model. As with PROSPECT,
 217 inversion based on iterative optimization can be considered. However, unlike PROSPECT
 218 inversion which is well-posed in most situations, PROSAIL inversion is inherently ill-posed.
 219 Therefore, standard iterative optimization algorithms consisting in minimizing a cost function
 220 will converge towards local minimum, unless global optimization algorithms are applied. This
 221 means that initial conditions of the iterative optimization influence the output of a local
 222 optimization.

223 Multiple inversion strategies based on iterative optimization are implemented in the package
 224 `prospect`. The main iterative optimization algorithm is based on the minimization of a
 225 multivariable function with nonlinear constraints. This procedure is based on the function
 226 `fmincon` included in the package `pracma`. The default criterion for the cost function corresponds
 227 to the root mean square error (RMSE) between a reference surface reflectance and surface
 228 reflectance simulated with PROSAIL. The code below provides an example of iterative
 229 optimization applied to simulated surface reflectance at native spectral sampling (1 nm),
 230 and to Sentinel-2 surface reflectance.

```
# define initial value, lower and upper bounds for inversion
init <- data.frame('chl' = 40, 'car' = 10, 'ewt' = 0.01, 'lma' = 0.01,
                     'lai' = 3, 'lidf_a' = 50, 'n_struct' = 1.5)
lb <- data.frame('chl' = 5, 'car' = 1, 'ewt' = 0.002, 'lma' = 0,
                  'lai' = 0.5, 'lidf_a' = 30, 'n_struct' = 1)
ub <- data.frame('chl' = 80, 'car' = 20, 'ewt' = 0.03, 'lma' = 0.03,
                  'lai' = 6, 'lidf_a' = 80, 'n_struct' = 3)

# define parameters set for inversion
parm_set <- data.frame('tts' = 40, 'tto' = 0, 'psi' = 60, 'soil_brightness' = 1,
                         'ant' = 0, 'brown' = 0, 'hotspot' = 0.1)

# define soil reflectance (set as prior knowledge) and spec_soil variable
rsoil <- parm_set$soil_brightness*spec_soil_oss$soil_01
spec_soil <- data.frame('lambda' = spec_soil$lambda,
                        'refl' = rsoil)

# simulate canopy surface reflectance with 1 nm sampling
truth <- data.frame('chl' = 60, 'car' = 8, 'ewt' = 0.015, 'lma' = 0.005,
                     'lai' = 3, 'lidf_a' = 60, 'n_struct' = 1.8)
```

```

refl_1nm <- prosail(n_struct = truth$n_struct, chl = truth$chl, car = truth$car,
                     ant = parm_set$ant, brown = parm_set$brown,
                     ewt = truth$ewt, lma = truth$lma, type_lidf = 2,
                     lai = truth$lai, hotspot = parm_set$hotspot,
                     lidf_a = init$lidf_a, rsoil = rsoil, tts = parm_set$tts,
                     tto = parm_set$tto, psi = parm_set$psi)
surf_refl_1nm <- get_surf_refl(rdot = refl_1nm$rdot, rsot = refl_1nm$rsot,
                                 tts = parm_set$tts,
                                 spec_atm_sensor = spec_atm)

# invert PROSAIL on surface reflectance with 1 nm spectral sampling
est_1nm <- invert_prosail(refl_mes = surf_refl_1nm$surf_refl,
                           initialization = init,
                           lower_bound = lb, upper_bound = ub, type_lidf = 2,
                           spec_prospect_sensor = spec_prospect_full_range,
                           spec_atm_sensor = spec_atm,
                           spec_soil_sensor = spec_soil,
                           parm_set = parm_set)

# convert spectral input based on Sentinel-2 SRF
srf_s2 <- get_srf_sensor(sensor_name = 'Sentinel_2A')
spec_prospect <- spec_prospect_full_range
lambda <- spec_prospect_full_range$lambda
surf_refl_S2 <- apply_sensor_characteristics(wvl = lambda,
                                              srf = srf_s2,
                                              refl = surf_refl_1nm$surf_refl)
spec_prospect_s2 <- apply_sensor_characteristics(wvl = lambda, srf = srf_s2,
                                                   refl = spec_prospect)
spec_soil_s2 <- apply_sensor_characteristics(wvl = lambda, srf = srf_s2,
                                               refl = spec_soil)
spec_atm_s2 <- apply_sensor_characteristics(wvl = lambda, srf = srf_s2,
                                              refl = spec_atm)

# invert PROSAIL on Sentinel-2 surface reflectance
est_s2 <- invert_prosail(refl_mes = surf_refl_S2, initialization = init,
                         lower_bound = lb, upper_bound = ub,
                         spec_prospect_sensor = spec_prospect_s2,
                         spec_atm_sensor = spec_atm_s2,
                         spec_soil_sensor = spec_soil_s2,
                         type_lidf = 2, parm_set = parm_set)

```

231 Iterative optimization with prior information

232 Prior information can be added to the cost function in order to regularize the ill-posed inverse
 233 problem ([Combal et al., 2003](#)). Multiple possibilities exist to account for prior information:

- 234 ▪ the definition of initialization variable according to initial assumptions
- 235 ▪ the addition of a term corresponding to the probability density function of part or all of
 236 the parameters to be estimated in the cost function.

237 The code blow illustrates the introduction of prior information on LIDF, with the definition of
 238 a probability density function corresponding to the average leaf angle lidf_a. A weighting
 239 factor associated to the relative importance of this prior information with respect to the main
 240 criterion to minimize (RMSE between reference surface reflectance and simulated surface
 241 reflectance) can also be adjusted.

```

# define prior information on average leaf angle lidf_a
prior_info <- list('mean' = data.frame('lidf_a' = 60),
                    'sd' = data.frame('lidf_a' = 10),
                    'weight_prior' = 0.01)

# invert PROSAIL on surface reflectance with 1 nm spectral sampling and
# probability density function for lidf_a
est_1nm_p <- invert_prosail(refl_mes = surf_refl_1nm$surf_refl,
                             initialization = init,
                             lower_bound = lb, upper_bound = ub,
                             spec_prospect_sensor = spec_prospect_full_range,
                             spec_atm_sensor = spec_atm,
                             spec_soil_sensor = spec_soil,
                             type_lidf = 2, parm_set = parm_set,
                             prior_info = prior_info)

# invert PROSAIL on Sentinel-2 surface reflectance and probability density
# function for lidf_a
est_s2_p <- invert_prosail(refl_mes = surf_refl_S2, initialization = init,
                            lower_bound = lb, upper_bound = ub,
                            spec_prospect_sensor = spec_prospect_s2,
                            spec_atm_sensor = spec_atm_s2,
                            spec_soil_sensor = spec_soil_s2,
                            type_lidf = 2, parm_set = parm_set,
                            prior_info = prior_info)

```

242 PROSAIL hybrid inversion

243 Hybrid model inversion is defined here as a two-step inversion procedure:

- 244 ■ run RTM to produce a simulated LUT including sensor surface reflectance and
 245 corresponding PROSAIL input parameters, including vegetation properties.
- 246 ■ train a machine learning regression algorithm to estimate a vegetation property or a set
 247 of vegetation properties of interest from sensor surface reflectance.

248 The next subsections describe the strategy followed by the hybrid inversion implemented in
 249 `prosail`.

250 Simulating surface reflectance to prepare for regression model training

251 Several factors need to be accounted for when preparing for the training stage of the regression
 252 models :

- 253 ■ the sampling strategy (range, distribution, co-distributions for input parameters)
 254 ■ the addition of additive and multiplicative noise to the simulated surface reflectance
 255 ■ the definition of spectral bands to be used for the training of the regression model

256 The default parameterization of `prosail` hybrid inversion relies on the production of a surface
 257 reflectance LUT compliant with the specifications defined in the ATBD for the Biophysical
 258 Processor of the Sentinel toolbox ([Weiss et al., 2020](#)). However, each step of the simulation
 259 of a training LUT can be defined by user.

260 Training a machine learning regression algorithm

261 The machine learning strategy implemented in `prosail` consists in a parsimonious ensemble
 262 method based on a bootstrap aggregating (bagging) prediction of biophysical properties from

multiple support vector regression (SVR) models. Each SVR model is trained with a limited number of samples, ensuring fast training stage. The predicted value then corresponds to the mean prediction from a set of SVR models. The standard deviation can also be derived from this ensemble of predictors. However, standard deviation may not provide accurate model uncertainty quantification (Palmer et al., 2022).

The default parameterization of this inversion strategy uses an ensemble of 10 SVR models, each of them trained with 200 samples. Therefore, only 2000 samples are required for the training stage, which is relatively low compared to the 41472 cases used for the training of the artificial neural networks used in the SNAP toolbox. This parsimonious ensemble method ensures very fast training stage and similar retrieval performances as those obtained with the SNAP toolbox.

Performing full hybrid inversion

Figure 1 summarizes the workflow applied to perform hybrid inversion. The function `train_prosail_inversion` combines all aforementioned steps to produce surface reflectance simulations and train SVR models. It provides regression models as outputs, which can then be directly used to estimate vegetation biophysical properties from data tables or raster data.

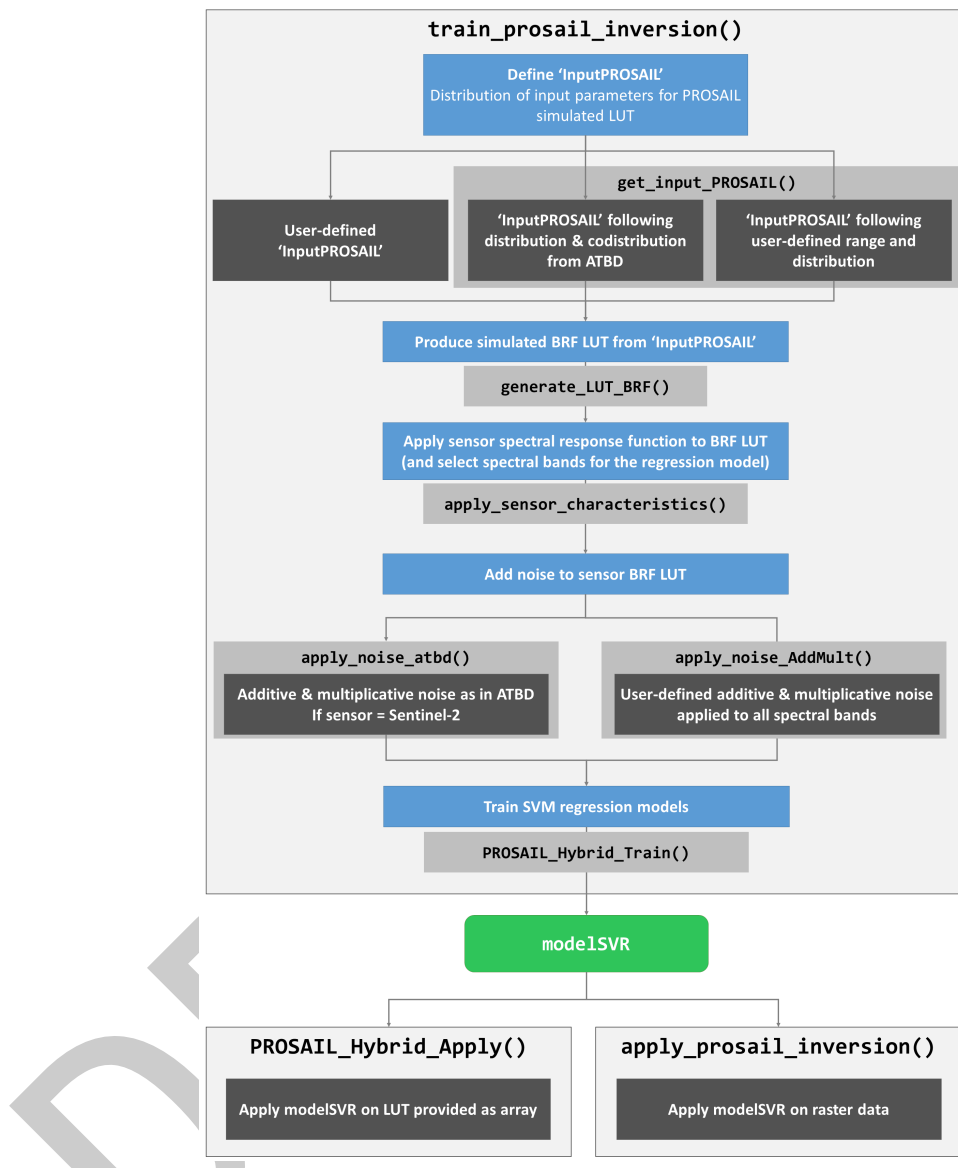


Figure 1: Workflow of PROSAIL hybrid inversion implemented in the package prosail.

279 The example code below illustrates the training stage with the function `train_prosail_inversion`,
 280 to estimate LAI, fCover and fAPAR from Sentinel-2, using the three spectral bands
 281 corresponding to green channel (B3), red channel (B4) and near infrared channel (B8) as
 282 specified in the ATBD document.

```

# define sensor to simulate with PROSAIL
srf <- get_srf_sensor(sensor_name = 'Sentinel_2')

# define parameters to estimate
parms_to_estimate <- c('lai', 'fcover', 'fapar')

# define spectral bands required to train SVR model for each variable
selected_bands <- list()
for (parm in parms_to_estimate)
  selected_bands[[parm]] <- c('B3', 'B4', 'B8')

```

```

# define output directory where LUTs will be saved
prosail_dir <- './hybrid_inversion'

# define ranges for geometry of acquisition
geom_acq <- list('min' = data.frame('tto' = 0, 'tts' = 20, 'psi' = 0),
                  'max' = data.frame('tto' = 10, 'tts' = 30, 'psi' = 360))

# train model
modelSVR <- train_prosail_inversion(parms_to_estimate = parms_to_estimate,
                                       atbd = TRUE, geom_acq = geom_acq,
                                       srf = srf, selected_bands = selected_bands,
                                       output_dir = prosail_dir)

```

283 The processing steps called in `train_prosail_inversion` can be broken down as follows:

```

# produce input variables following ATBD specifications and geometry of acq.
input_prosail <- get_input_prosail(atbd = TRUE, geom_acq = geom_acq)

# generate a LUT with 1 nm spectral sampling
res <- generate_lut_prosail(SAILversion = '4SAIL',
                            input_prosail = input_prosail,
                            spec_prospect = spec_prospect_full_range,
                            spec_soil = spec_soil_atbd_v2, spec_atm = spec_atm)

# include fcover and fAPAR (derived from SAIL reflectance / absorption factors)
# in the pool of variables to explain
input_prosail$fcover <- res$fcover
input_prosail$fapar <- res$fapar

# apply Sentinel-2 SRF to get sensor surface reflectance
surf_refl_LUT <- apply_sensor_characteristics(wvl = lambda, srf = srf,
                                                refl = res$surf_refl)

# identify spectral bands in LUT
rownames(surf_refl_LUT) <- srf$spectral_bands

# apply noise and produce a LUT for each parameter
surf_refl_noise <- list()
for (parm in parms_to_estimate)
  surf_refl_noise[[parm]] <- apply_noise_atbd(refl_lut = surf_refl_LUT)

# train a set of SVR models for each parameter
modelSVR <- list()
for (parm in parms_to_estimate){
  input_variables <- input_prosail[[parm]]
  modelSVR[[parm]] <- prosail_hybrid_train(refl_lut = surf_refl_noise[[parm]],
                                             input_variables = input_variables)
}

```

284 The resulting models can then be applied on data tables or raster data. The following example
 285 perform predictions based on models trained previously. The prediction returns mean value
 286 obtained form the ensemble of regression models for each sample, as well as corresponding
 287 standard deviation.

```

mean_estimate <- sd_estimate <- list()
for (parm in parms_to_estimate){
  HybridRes <- prosail_hybrid_apply(regression_models = modelSVR[[parm]],

```

```

    refl = surf_refl_noise[[parm]])
mean_estimate[[parm]] <- HybridRes$mean_estimate
sd_estimate[[parm]] <- HybridRes$sd_estimate
}

```

288 Application to imagery data

289 Here, we illustrate how to run prosail hybrid inversion on Sentinel-2 imagery. Sentinel-2
 290 imagery handling requires the installation of `preprocs2`, a package dedicated to downloading
 291 and preprocessing of Sentinel-2 data from different providers. It also requires the package `sf`
 292 to handle vector data.

293 Here, for the sake of comparison between biophysical variables produced from SNAP and those
 294 produced with the prosail hybrid inversion, the Sentinel-2 Level-2A product corresponding to
 295 tile *30SWJ* acquired on *May 13th, 2021* was downloaded from the Copernicus Data Space
 296 Ecosystem ([CDSE](#)). This is important for the consistency of the processing baseline of Sentinel-
 297 2 acquisitions, as the processing baseline used by alternative Sentinel-2 data providers such
 298 as Microsoft Planetary Computers and Google Cloud may not be consistent with the latest
 299 version provided by CDSE.

300 Users are invited to go through the documentation of the package `prosail`, which provides
 301 examples on how to download Sentinel-2 imagery data from specific regions of interest instead
 302 of downloading a full SAFE tile.

303 Once the SAFE product downloaded `preprocs2` is used to crop and save reflectance data
 304 corresponding to an area of interest defined within the Sentinel-2 tile footprint.

```

# load preprocS2 and sf
library(preprocS2)
library(sf)
# define path for original image subset and prosail outputs
main_dir <- './barrax'                                # main directory
safe_dir <- file.path(main_dir, 's2_safe')             # SAFE directory
out_s2 <- file.path(main_dir, 'S2_subset')              # S2 subset directory
out_BP <- file.path(main_dir, 'prosail_inversion')      # prosail products directory

# search for L2A scene of interest with sen2proc
stac_items <- s2_search(start = "2021-05-13", level = "L2A", tile = "30SWJ")

# download files with sen2proc
dir.create(path = safe_dir, showWarnings = FALSE, recursive = TRUE)
safe_path <- cdse_download(x = stac_items, outdir = safe_dir)

# define area of interest included in S2 tile
aoi_bbox <- st_bbox(obj = c('xmin' = 571626, 'ymin' = 4324941,
                           'xmax' = 582995, 'ymax' = 4331253))
aoi <- bbox_to_poly(aoi_bbox, crs = 32630)
path_aoi <- file.path(main_dir, 'barrax.gpkg')
st_write(obj = aoi, dsn = path_aoi, driver = 'GPKG', delete_dsn = T)

# extract area of interest from SAFE with preprocS2
s2_products <- extract_from_safe(safe_path = safe_path,
                                   path_aoi = path_aoi,
                                   output_dir = out_s2)
raster_path <- s2_products$Refl_path
mask_path <- s2_products$cloudmasks$BinaryMask

```

305 The resulting raster data can then be directly processed with prosail using the code provided
 306 hereafter.

```

# get geometry of acquisition with preprocS2
s2_geom <- get_s2_geometry(MTD_TL_xml = s2_products$MTD_TL)
geom_acq <- list('min' = data.frame('tto' = min(s2_geom$VZA, na.rm = T),
                                'tts' = min(s2_geom$SZA, na.rm = T),
                                'psi' = min(abs(s2_geom$SAA-s2_geom$VAA),
                                            na.rm = T)),
                  'max' = data.frame('tto' = max(s2_geom$VZA, na.rm = T),
                                     'tts' = max(s2_geom$SZA, na.rm = T),
                                     'psi' = max(abs(s2_geom$SAA-s2_geom$VAA),
                                                 na.rm = T)))
# get sensor response for Sentinel-2
srf <- get_srf_sensor(sensor_name = 'Sentinel_2B')
band_names <- srf$spectral_bands

# define parameters to estimate
parms_to_estimate <- c('lai', 'fcover', 'fapar', 'chl')

# define spectral bands required to train SVR model for each variable
selected_bands <- list('lai' = c('B3', 'B4', 'B8'),
                        'fcover' = c('B3', 'B4', 'B8'),
                        'fapar' = c('B3', 'B4', 'B8'),
                        'chl' = c('B3', 'B4', 'B5', 'B6', 'B7', 'B8'))

# train SVR model for each variable of interest
modelSVR <- train_prosail_inversion(parms_to_estimate = parms_to_estimate,
                                       atbd = TRUE, geom_acq = geom_acq,
                                       srf = srf,
                                       selected_bands = selected_bands,
                                       output_dir = out_BP)

# apply SVR on S2 L2A reflectance
options <- set_options_prosail(fun = 'apply_prosail_inversion')
options$multiplying_factor <- 10000
options$tiling <- TRUE
BPvars <- apply_prosail_inversion(raster_path = raster_path,
                                   mask_path = mask_path,
                                   hybrid_model = modelSVR,
                                   output_dir = out_BP,
                                   band_names = band_names,
                                   selected_bands = selected_bands,
                                   options = options)

```

307 Comparison with SNAP toolbox

308 LAI, fcover and fAPAR computed from Sentinel-2 images with the hybrid inversion implemented
 309 in prosail are compared to those produced with SNAP in Figure 2.

Biophysical properties estimated with prosail vs Biophysical properties estimated with SNAP.

Figure 2: Biophysical properties estimated with prosail vs Biophysical properties estimated with SNAP.

310 The two methods show relatively good consistency with Pearson correlation coefficient ranging

311 between 0.99 and 1.00 for LAI, and superior to 0.97 for fCover and fAPAR. Algorithmic
312 differences remain between the results obtained from the biophysical processor of the SNAP
313 toolbox and the inversion obtained with prosail, including: - the version of the PROSPECT
314 model: SNAP uses a version anterior to PROSPECT-D, - the machine learning algorithm.
315 The differences in the retrieval of the vegetation biophysical properties suggest differences in
316 the soil properties accounted for in simulations with low LAI, despite our efforts to reproduce
317 the workflow described in the ATBD (Weiss et al., 2020). Additional tests performed over
318 other sites (on both croplands and forests) showed similar performances.
319 The availability of open source and fully parameterizable inversion procedures should contribute
320 to improve reproducibility of currently available softwares.

321 Conclusion

322 We introduce prosail, an R package dedicated to the canopy reflectance model PROSAIL,
323 coupling PROSPECT and SAIL. prosail is coupled with the R package prospect in order
324 to allow seamless integration of future versions of the leaf model. It allows simulation of
325 bi-directional reflectance factor and surface reflectance for any type of optical sensor based on
326 their spectral response, including multispectral sensors and hyperspectral sensors. The package
327 also includes a collection of inversion procedures, including iterative optimization with and
328 without prior information, and hybrid inversion.
329 The estimation of vegetation biophysical properties with prosail hybrid inversion is consistent
330 with estimations produced with the method implemented in the Sentinel toolbox, which is
331 currently the reference method.
332 prosail hybrid inversion does not intend to be computationally as efficient as SNAP and
333 may not meet requirements for large scale vegetation monitoring applications. prosail hybrid
334 inversion offers a fully adjustable hybrid inversion framework, including an original parsimonious
335 machine learning regression method, allowing fast and efficient training for any type of sensor.
336 It is a valuable tool for experimenting on the potential and limitation of physically-based
337 retrieval of vegetation traits from various types of optical sensors, including airborne imaging
338 spectroscopy, as well satellite missions already operational and in preparation.

339 Availability

340 prosail is an open-source software package made available under the MIT license. Tutorials
341 are available at <https://jbferet.gitlab.io/prosail/>.

342 Acknowledgements

343 The authors acknowledge financial support from Agence Nationale de la Recherche (BioCop
344 project — ANR-17-CE32-0001). We are grateful to Wout Verhoef for the development of the
345 initial version of the 4SAIL and 4SAIL2 models. We are grateful to Stéphane Jacquemoud and
346 Frédéric Baret for the development of the initial version of the prospect model.

347 AI Usage Disclosure

348 No generative AI tools were used in the development of this software, the writing of this
349 manuscript, or the preparation of supporting materials.

References

- 350 Berger, K., Atzberger, C., Danner, M., D'Urso, G., Mauser, W., Vuolo, F., & Hank, T. (2018).
 352 Evaluation of the PROSAIL model capabilities for future hyperspectral model environments:
 353 A review study. *Remote Sensing*, 10(1). <https://doi.org/10.3390/rs10010085>
- 354 Bréon, F.-M., Maignan, F., Leroy, M., & Grant, I. (2002). Analysis of hot spot directional
 355 signatures measured from space. *Journal of Geophysical Research: Atmospheres*, 107(D16),
 356 AAC 1-1-AAC 1-15. <https://doi.org/10.1029/2001JD001094>
- 357 C. François, C. Ottlé, A. Olioso, L. Prévot, N. Bruguier, & Y. Ducros. (2002). Conversion
 358 of 400-1100 nm vegetation albedo measurements into total shortwave broadband albedo
 359 using a canopy radiative transfer model. *Agronomie*, 22(6), 611–618. <https://doi.org/10.1051/agro:2002033>
- 360 Caicedo, J. P. R., Verrelst, J., Muñoz-Marí, J., Moreno, J., & Camps-Valls, G. (2014). Toward
 361 a semiautomatic machine learning retrieval of biophysical parameters. *IEEE Journal of
 362 Selected Topics in Applied Earth Observations and Remote Sensing*, 7(4), 1249–1259.
 363 <https://doi.org/10.1109/JSTARS.2014.2298752>
- 364 Campbell, G. S. (1990). Derivation of an angle density function for canopies with ellipsoidal
 365 leaf angle distributions. *Agricultural and Forest Meteorology*, 49(3), 173–176. [https://doi.org/10.1016/0168-1923\(90\)90030-A](https://doi.org/10.1016/0168-1923(90)90030-A)
- 366 Combal, B., Baret, F., Weiss, M., Trubuil, A., Macé, D., Pragnère, A., Myneni, R., Knyazikhin,
 367 Y., & Wang, L. (2003). Retrieval of canopy biophysical variables from bidirectional
 368 reflectance: Using prior information to solve the ill-posed inverse problem. *Remote Sensing
 369 of Environment*, 84(1), 1–15. [https://doi.org/10.1016/S0034-4257\(02\)00035-4](https://doi.org/10.1016/S0034-4257(02)00035-4)
- 370 Féret, J.-B., Berger, K., Boissieu, F. de, & Malenovský, Z. (2021). PROSPECT-PRO for
 371 estimating content of nitrogen-containing leaf proteins and other carbon-based constituents.
 372 *Remote Sensing of Environment*, 252, 112173. <https://doi.org/10.1016/j.rse.2020.112173>
- 373 Féret, J.-B., & Boissieu, F. de. (2024). Prospect: An r package to link leaf optical properties
 374 with their chemical and structural properties with the leaf model PROSPECT. *Journal of
 375 Open Source Software*, 9(94), 6027. <https://doi.org/10.21105/joss.06027>
- 376 Féret, J.-B., Boissieu, F. de, & Lang, M. (2026). A plant trait-based approach to map forest
 377 biodiversity using imaging spectroscopy and physical modeling. In D. Rocchini (Ed.), *R
 378 coding for ecology* (pp. 161–182). Springer Nature Switzerland. https://doi.org/10.1007/978-3-031-99665-8_7
- 379 Féret, J.-B., Gitelson, A. A., Noble, S. D., & Jacquemoud, S. (2017). PROSPECT-D:
 380 Towards modeling leaf optical properties through a complete lifecycle. *Remote Sensing of
 381 Environment*, 193, 204–215. <https://doi.org/10.1016/j.rse.2017.03.004>
- 382 Féret, J.-B., le Maire, G., Jay, S., Berveiller, D., Bendoula, R., Hmimina, G., Cheraiet, A.,
 383 Oliveira, J. C., Ponzoni, F. J., Solanki, T., de Boissieu, F., Chave, J., Nouvellon, Y.,
 384 Porcar-Castell, A., Proisy, C., Soudani, K., Gastellu-Etchegorry, J.-P., & Lefèvre-Fonolloza,
 385 M.-J. (2019). Estimating leaf mass per area and equivalent water thickness based on leaf
 386 optical properties: Potential and limitations of physical modeling and machine learning.
 387 *Remote Sensing of Environment*, 231, 110959. <https://doi.org/10.1016/j.rse.2018.11.002>
- 388 Ferreira, V. B., Féret, J.-B., Atzberger, C., Guillemot, J., Campoe, O., & Maire, G. le. (2026).
 389 Enhancing PROSAIL inversion: Key considerations and practical insights. *IEEE Journal
 390 of Selected Topics in Applied Earth Observations and Remote Sensing*, 19, 1378–1390.
 391 <https://doi.org/10.1109/JSTARS.2025.3635001>
- 392 Gastellu-Etchegorry, J.-P., Yin, T., Lauret, N., Cajgfinger, T., Gregoire, T., Grau, E., Féret,
 393 J.-B., Lopes, M., Guilleux, J., Dedieu, G., Malenovský, Z., Cook, B. D., Morton, D., Rubio,
 394 J., & de Boissieu. (2026). prosail: an R package to simulate canopy reflectance with the coupled model PROSAIL (PROSPECT + SAIL)16
 395 *Journal of Open Source Software*, 16(VOL? (ISSUE?)), 9921. <https://doi.org/10.4236/jos.9921>

- 397 J., Durrieu, S., Cazanave, G., Martin, E., & Ristorcelli, T. (2015). Discrete anisotropic
 398 radiative transfer (DART 5) for modeling airborne and satellite spectroradiometer and
 399 LIDAR acquisitions of natural and urban landscapes. *Remote Sensing*, 7(2), 1667–1701.
 400 <https://doi.org/10.3390/rs70201667>
- 401 Hauser, L. T., Féret, J.-B., An Binh, N., van der Windt, N., Sil, Å. F., Timmermans, J.,
 402 Soudzilovskaia, N. A., & van Bodegom, P. M. (2021). Towards scalable estimation of plant
 403 functional diversity from sentinel-2: In-situ validation in a heterogeneous (semi-)natural
 404 landscape. *Remote Sensing of Environment*, 262, 112505. <https://doi.org/10.1016/j.rse.2021.112505>
- 405 Hijmans, R. J. (2025). *Terra: Spatial data analysis*. <https://CRAN.R-project.org/package=terra>
- 406 Jacquemoud, S., & Baret, F. (1990). PROSPECT: A model of leaf optical properties
 407 spectra. *Remote Sensing of Environment*, 34(2), 75–91. [https://doi.org/10.1016/0034-4257\(90\)90100-Z](https://doi.org/10.1016/0034-4257(90)90100-Z)
- 408 Jacquemoud, S., Verhoef, W., Baret, F., Bacour, C., Zarco-Tejada, P. J., Asner, G. P.,
 409 François, C., & Ustin, S. L. (2009). PROSPECT+SAIL models: A review of use for
 410 vegetation characterization. *Remote Sensing of Environment*, 113, S56–S66. <https://doi.org/10.1016/j.rse.2008.01.026>
- 411 Kuusk, A. (1991). The hot spot effect in plant canopy reflectance. In R. B. Mynden & J. Ross
 412 (Eds.), *Photon-vegetation interactions: Applications in optical remote sensing and plant*
 413 *ecology* (pp. 139–159). Springer Berlin Heidelberg. https://doi.org/10.1007/978-3-642-75389-3_5
- 414 Palmer, G., Du, S., Politowicz, A., Emory, J. P., Yang, X., Gautam, A., Gupta, G., Li, Z.,
 415 Jacobs, R., & Morgan, D. (2022). Calibration after bootstrap for accurate uncertainty
 416 quantification in regression models. *Npj Computational Materials*, 8(1), 115. <https://doi.org/10.1038/s41524-022-00794-8>
- 417 Poulter, B., Currey, B., Calle, L., Shiklomanov, A. N., Amaral, C. H., Brookshire, E. N. J.,
 418 Campbell, P., Chlus, A., Cawse-Nicholson, K., Huemmrich, F., Miller, C. E., Miner, K.,
 419 Pierrat, Z., Raiho, A. M., Schimel, D., Serbin, S., Smith, W. K., Stavros, N., Stutz, J., ...
 420 Zhang, Z. (2023). Simulating global dynamic surface reflectances for imaging spectroscopy
 421 spaceborne missions: LPJ-PROSAIL. *Journal of Geophysical Research: Biogeosciences*,
 422 128(1), e2022JG006935. <https://doi.org/10.1029/2022JG006935>
- 423 Spafford, L., le Maire, G., MacDougall, A., de Boissieu, F., & Féret, J.-B. (2021). Spectral
 424 subdomains and prior estimation of leaf structure improves PROSPECT inversion on
 425 reflectance or transmittance alone. *Remote Sensing of Environment*, 252, 112176. <https://doi.org/10.1016/j.rse.2020.112176>
- 426 Spitters, C. J. T., Toussaint, H. A. J. M., & Goudriaan, J. (1986). Separating the diffuse and
 427 direct component of global radiation and its implications for modeling canopy photosynthesis
 428 part i. Components of incoming radiation. *Agricultural and Forest Meteorology*, 38(1),
 429 217–229. [https://doi.org/10.1016/0168-1923\(86\)90060-2](https://doi.org/10.1016/0168-1923(86)90060-2)
- 430 Verhoef, W. (1984). Light scattering by leaf layers with application to canopy reflectance
 431 modeling: The SAIL model. *Remote Sensing of Environment*, 16(2), 125–141. [https://doi.org/10.1016/0034-4257\(84\)90057-9](https://doi.org/10.1016/0034-4257(84)90057-9)
- 432 Verhoef, W. (1998). *Theory of radiative transfer models applied in optical remote sensing*
 433 *of vegetation canopies : E-book* [PhD Thesis - Research external, graduation external].
 434 Landbouwuniversiteit Wageningen (LUW). ISBN: 90-5485-804-4
- 435 Verhoef, Wout, & Bach, H. (2007). Coupled soil–leaf-canopy and atmosphere radiative transfer
 436 modeling to simulate hyperspectral multi-angular surface reflectance and TOA radiance
 437 data. *Remote Sensing of Environment*, 109(2), 166–182. <https://doi.org/10.1016/j.rse.2007.06.011>

446 2006.12.013

- 447 Verhoef, W., Jia, L., Xiao, Q., & Su, Z. (2007). Unified optical-thermal four-stream radiative
448 transfer theory for homogeneous vegetation canopies. *IEEE Transactions on Geoscience
449 and Remote Sensing*, 45(6), 1808–1822. <https://doi.org/10.1109/TGRS.2007.895844>
- 450 Verrelst, J., Camps-Valls, G., Muñoz-Marí, J., Rivera, J. P., Veroustraete, F., Clevers, J. G. P.
451 W., & Moreno, J. (2015). Optical remote sensing and the retrieval of terrestrial vegetation
452 bio-geophysical properties – a review. *ISPRS Journal of Photogrammetry and Remote
453 Sensing*, 108, 273–290. <https://doi.org/10.1016/j.isprsjprs.2015.05.005>
- 454 Weiss, M., Baret, F., & Jay, S. (2020). *S2ToolBox Level 2 products LAI, FAPAR, FCover*
455 [Research Report]. EMMAH-CAPTE, INRAe Avignon. <https://hal.inrae.fr/hal-03584016>
- 456 Yang, P., Prikaziuk, E., Verhoef, W., & Tol, C. van der. (2021). SCOPE 2.0: A model
457 to simulate vegetated land surface fluxes and satellite signals. *Geoscientific Model
458 Development*, 14(7), 4697–4712. <https://doi.org/10.5194/gmd-14-4697-2021>

DRAFT